A Programmable Dual-RNA–Guided DNA Endonuclease in Adaptive Bacterial Immunity

Martin Jinek,[1,2]* Krzysztof Chylinski,[3,4]* Ines Fonfara,[4] Michael Hauer,[2]† Jennifer A. Doudna,[1,2,5,6]‡ Emmanuelle Charpentier[4]‡

Clustered regularly interspaced short palindromic repeats (CRISPR)/CRISPR-associated (Cas) systems provide bacteria and archaea with adaptive immunity against viruses and plasmids by using CRISPR RNAs (crRNAs) to guide the silencing of invading nucleic acids. We show here that in a subset of these systems, the mature crRNA that is base-paired to trans-activating crRNA (tracrRNA) forms a two-RNA structure that directs the CRISPR-associated protein Cas9 to introduce double-stranded (ds) breaks in target DNA. At sites complementary to the crRNA-guide sequence, the Cas9 HNH nuclease domain cleaves the complementary strand, whereas the Cas9 RuvC-like domain cleaves the noncomplementary strand. The dual-tracrRNA:crRNA, when engineered as a single RNA chimera, also directs sequence-specific Cas9 dsDNA cleavage. Our study reveals a family of endonucleases that use dual-RNAs for site-specific DNA cleavage and highlights the potential to exploit the system for RNA-programmable genome editing.

Bacteria and archaea have evolved RNA-mediated adaptive defense systems called clustered regularly interspaced short palindromic repeats (CRISPR)/CRISPR-associated (Cas) that protect organisms from invading viruses and plasmids (*1*–*3*). These defense systems rely on small RNAs for sequence-specific detection and silencing of foreign nucleic acids. CRISPR/Cas systems are composed of *cas* genes organized in operon(s) and CRISPR array(s) consisting of genome-targeting sequences (called spacers) interspersed with identical repeats (*1*–*3*). CRISPR/Cas-mediated immunity occurs in three steps. In the adaptive phase, bacteria and archaea harboring one or more CRISPR loci respond to viral or plasmid challenge by integrating short fragments of foreign sequence (protospacers) into the host chromosome at the proximal end of the CRISPR array (*1*–*3*). In the expression and interference phases, transcription of the repeat-spacer element into precursor CRISPR RNA (pre-crRNA) molecules followed by enzymatic cleavage yields the short crRNAs that can pair with complementary protospacer sequences of invading viral or plasmid targets (*4*–*11*). Target recognition by crRNAs directs the silencing of the foreign sequences by means of Cas proteins that function in complex with the crRNAs (*10*, *12*–*20*).

There are three types of CRISPR/Cas systems (*21*–*23*). The type I and III systems share some overarching features: specialized Cas endonucleases process the pre-crRNAs, and once mature, each crRNA assembles into a large multi-Cas protein complex capable of recognizing and cleaving nucleic acids complementary to the crRNA. In contrast, type II systems process pre-crRNAs by a different mechanism in which a trans-activating crRNA (tracrRNA) complementary to the repeat sequences in pre-crRNA triggers processing by the double-stranded (ds) RNA-specific ribonuclease RNase III in the presence of the Cas9 (formerly Csn1) protein (fig. S1) (*4*, *24*). Cas9 is thought to be the sole protein responsible for crRNA-guided silencing of foreign DNA (*25*–*27*).

We show here that in type II systems, Cas9 proteins constitute a family of enzymes that require a base-paired structure formed between the activating tracrRNA and the targeting crRNA to cleave target dsDNA. Site-specific cleavage occurs at locations determined by both base-pairing complementarity between the crRNA and the target protospacer DNA and a short motif [referred to as the protospacer adjacent motif (PAM)] juxtaposed to the complementary region in the target DNA. Our study further demonstrates that the Cas9 endonuclease family can be programmed with single RNA molecules to cleave specific DNA sites, thereby raising the exciting possibility of developing a simple and versatile RNA-directed system to generate dsDNA breaks for genome targeting and editing.

Cas9 is a DNA endonuclease guided by two RNAs. Cas9, the hallmark protein of type II systems, has been hypothesized to be involved in both crRNA maturation and crRNA-guided DNA interference (fig. S1) (*4*, *25*–*27*). Cas9 is involved in crRNA maturation (*4*), but its direct participation in target DNA destruction has not been investigated. To test whether and how Cas9 might be capable of target DNA cleavage, we used an overexpression system to purify Cas9 protein derived from the pathogen *Streptococcus pyogenes* (fig. S2, see supplementary materials and methods) and tested its ability to cleave a plasmid DNA or an oligonucleotide duplex bearing a protospacer sequence complementary to a mature crRNA, and a bona fide PAM. We found that mature crRNA alone was incapable of directing Cas9-catalyzed plasmid DNA cleavage (Fig. 1A and fig. S3A). However, addition of tracrRNA, which can pair with the repeat sequence of crRNA and is essential to crRNA maturation in this system, triggered Cas9 to cleave plasmid DNA (Fig. 1A and fig. S3A). The cleavage reaction required both magnesium and the presence of a crRNA sequence complementary to the DNA; a crRNA capable of tracrRNA base pairing but containing a noncognate target DNA-binding sequence did not support Cas9-catalyzed plasmid cleavage (Fig. 1A; fig. S3A, compare crRNA-sp2 to crRNA-sp1; and fig. S4A). We obtained similar results with a short linear dsDNA substrate (Fig. 1B and fig. S3, B and C). Thus, the trans-activating tracrRNA is a small noncoding RNA with two critical functions: triggering pre-crRNA processing by the enzyme RNase III (*4*) and subsequently activating crRNA-guided DNA cleavage by Cas9.

Cleavage of both plasmid and short linear dsDNA by tracrRNA:crRNA-guided Cas9 is site-specific (Fig. 1, C to E, and fig. S5, A and B). Plasmid DNA cleavage produced blunt ends at a position three base pairs upstream of the PAM sequence (Fig. 1, C and E, and fig. S5, A and C) (*26*). Similarly, within short dsDNA duplexes, the DNA strand that is complementary to the target-binding sequence in the crRNA (the complementary strand) is cleaved at a site three base pairs upstream of the PAM (Fig. 1, D and E, and fig. S5, B and C). The noncomplementary DNA strand is cleaved at one or more sites within three to eight base pairs upstream of the PAM. Further investigation revealed that the noncomplementary strand is first cleaved endonucleolytically and subsequently trimmed by a 3′-5′ exonuclease activity (fig. S4B). The cleavage rates by Cas9 under single-turnover conditions ranged from 0.3 to 1 min^{-1}, comparable to those of restriction endonucleases (fig. S6A), whereas incubation of wild-type (WT) Cas9-tracrRNA:crRNA complex with a fivefold molar excess of substrate DNA provided evidence that the dual-RNA–guided Cas9 is a multiple-turnover enzyme (fig. S6B). In

[1]Howard Hughes Medical Institute (HHMI), University of California, Berkeley, CA 94720, USA. [2]Department of Molecular and Cell Biology, University of California, Berkeley, CA 94720, USA. [3]Max F. Perutz Laboratories (MFPL), University of Vienna, A-1030 Vienna, Austria. [4]The Laboratory for Molecular Infection Medicine Sweden, Umeå Centre for Microbial Research, Department of Molecular Biology, Umeå University, S-90187 Umeå, Sweden. [5]Department of Chemistry, University of California, Berkeley, CA 94720, USA. [6]Physical Biosciences Division, Lawrence Berkeley National Laboratory, Berkeley, CA 94720, USA.

*These authors contributed equally to this work.
†Present address: Friedrich Miescher Institute for Biomedical Research, 4058 Basel, Switzerland.
‡To whom correspondence should be addressed. E-mail: doudna@berkeley.edu (J.A.D.); emmanuelle.charpentier@mims.umu.se (E.C.)

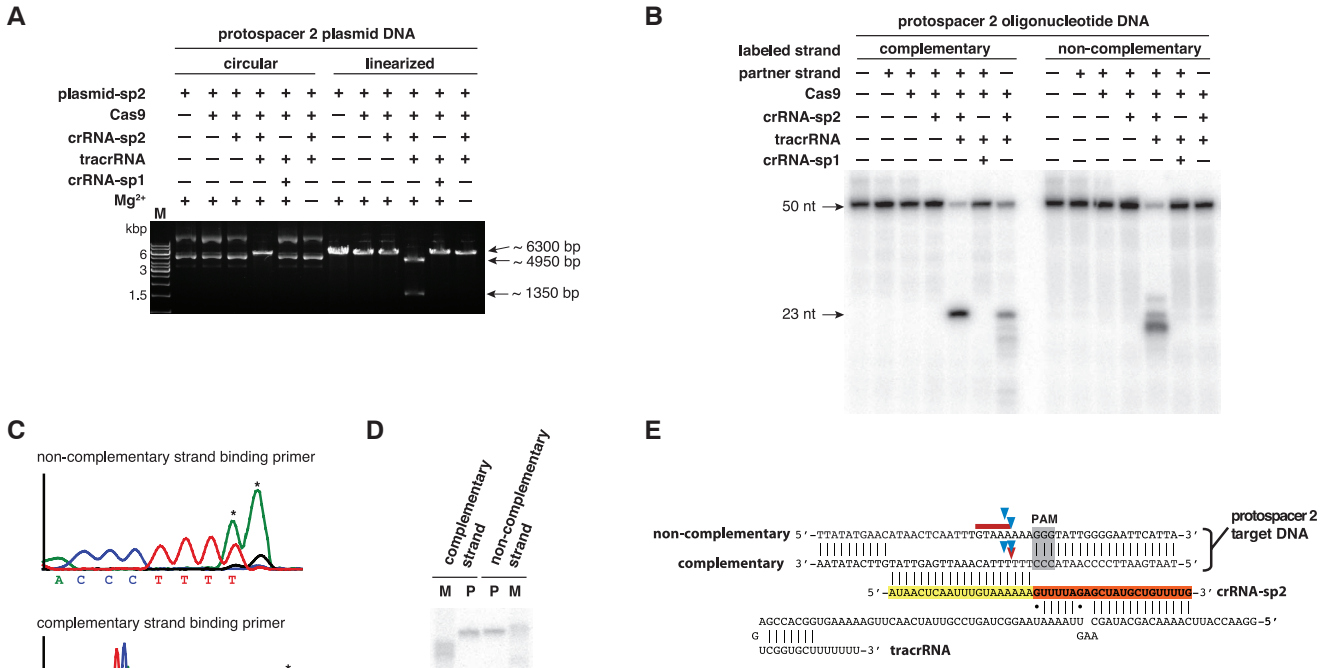

Fig. 1. Cas9 is a DNA endonuclease guided by two RNA molecules. (**A**) Cas9 was programmed with a 42-nucleotide crRNA-sp2 (crRNA containing a spacer 2 sequence) in the presence or absence of 75-nucleotide tracrRNA. The complex was added to circular or XhoI-linearized plasmid DNA bearing a sequence complementary to spacer 2 and a functional PAM. crRNA-sp1, specificity control; M, DNA marker; kbp, kilo–base pair. See fig. S3A. (**B**) Cas9 was programmed with crRNA-sp2 and tracrRNA (nucleotides 4 to 89). The complex was incubated with double- or single-stranded DNAs harboring a sequence complementary to spacer 2 and a functional PAM (*4*). The complementary or noncomplementary strands of the DNA were 5′-radiolabeled and annealed with a nonlabeled partner strand. nt, nucleotides. See fig. S3, B and C. (**C**) Sequencing analysis of cleavage products from Fig. 1A. Termination of primer extension in the sequencing reaction indicates the position of the cleavage site. The 3′ terminal A overhang (asterisks) is an artifact of the sequencing reaction. See fig. S5, A and C. (**D**) The cleavage products from Fig. 1B were analyzed alongside 5′ end-labeled size markers derived from the complementary and noncomplementary strands of the target DNA duplex. M, marker; P, cleavage product. See fig. S5, B and C. (**E**) Schematic representation of tracrRNA, crRNA-sp2, and protospacer 2 DNA sequences. Regions of crRNA complementarity to tracrRNA (orange) and the protospacer DNA (yellow) are represented. The PAM sequence is shown in gray; cleavage sites mapped in (C) and (D) are represented by blue arrows (C), a red arrow [(D), complementary strand], and a red line [(D), noncomplementary strand].

contrast to the CRISPR type I Cascade complex (*18*), Cas9 cleaves both linearized and supercoiled plasmids (Figs. 1A and 2A). Therefore, an invading plasmid can, in principle, be cleaved multiple times by Cas9 proteins programmed with different crRNAs.

Each Cas9 nuclease domain cleaves one DNA strand. Cas9 contains domains homologous to both HNH and RuvC endonucleases (Fig. 2A and fig. S7) (*21*–*23*, *27*, *28*). We designed and purified Cas9 variants containing inactivating point mutations in the catalytic residues of either the HNH or RuvC-like domains (Fig. 2A and fig. S7) (*23*, *27*). Incubation of these variant Cas9 proteins with native plasmid DNA showed that dual-RNA–guided mutant Cas9 proteins yielded nicked open circular plasmids, whereas the WT Cas9 protein-tracrRNA:crRNA complex produced a linear DNA product (Figs. 1A and 2A and figs. S3A and S8A). This result indicates that the Cas9 HNH and RuvC-like domains each cleave one plasmid DNA strand. To determine which strand of the target DNA is cleaved by each Cas9 catalytic domain, we incubated the mutant Cas9-tracrRNA:crRNA complexes with short dsDNA substrates in which either the complementary or noncomplementary strand was radiolabeled at its 5′ end. The resulting cleavage products indicated that the Cas9 HNH domain cleaves the complementary DNA strand, whereas the Cas9 RuvC-like domain cleaves the noncomplementary DNA strand (Fig. 2B and fig. S8B).

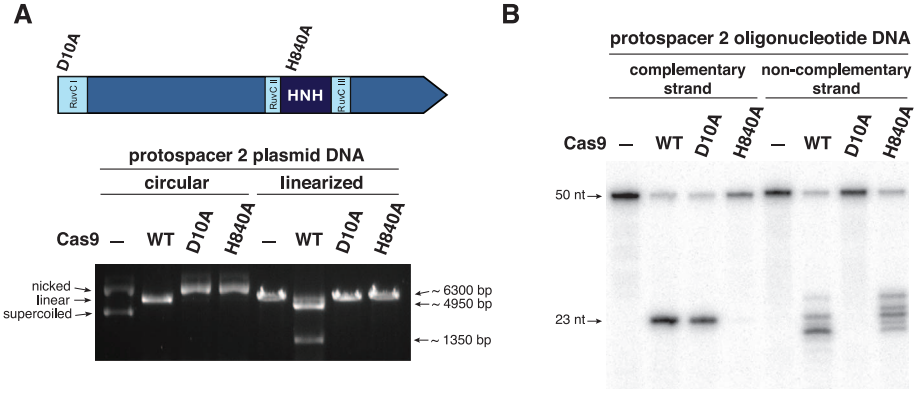

Fig. 2. Cas9 uses two nuclease domains to cleave the two strands in the target DNA. (**A**) (Top) Schematic representation of Cas9 domain structure showing the positions of domain mutations. D10A, Asp^{10}→Ala^{10}; H840A; His^{840}→Ala^{840}. (Bottom) Complexes of WT or nuclease mutant Cas9 proteins with tracrRNA: crRNA-sp2 were assayed for endonuclease activity as in Fig. 1A. (**B**) Complexes of WT Cas9 or nuclease domain mutants with tracrRNA and crRNA-sp2 were tested for activity as in Fig. 1B.

Dual-RNA requirements for target DNA binding and cleavage. tracrRNA might be required for target DNA binding and/or to stimulate the nuclease activity of Cas9 downstream of target recognition. To distinguish between these possibilities, we used an electrophoretic mobility shift assay to monitor target DNA binding by catalytically inactive Cas9 in the presence or absence of crRNA and/or tracrRNA. Addition of tracrRNA substantially enhanced target DNA binding by Cas9, whereas we observed little specific DNA binding with Cas9 alone or Cas9-crRNA (fig. S9). This indicates that tracrRNA is required for target DNA recognition, possibly by properly orienting the crRNA for interaction with the complementary strand of target DNA. The predicted tracrRNA:crRNA secondary structure includes base pairing between the 22 nucleotides at the 3′ terminus of the crRNA and a segment near the 5′ end of the mature tracrRNA (Fig. 1E). This interaction creates a structure in which the 5′-terminal 20 nucleotides of the crRNA, which vary in sequence in different crRNAs, are available for target DNA binding. The bulk of the tracrRNA downstream of the crRNA base-pairing region is free to form additional RNA structure(s) and/or to interact with Cas9 or the target DNA site. To determine whether the entire length of the tracrRNA is necessary for site-specific Cas9-catalyzed DNA cleavage, we tested Cas9-tracrRNA:crRNA complexes reconstituted using full-length mature (42-nucleotide) crRNA and various truncated forms of tracrRNA lacking sequences at their 5′ or 3′ ends. These complexes were tested for cleavage using a short target dsDNA. A substantially truncated version of the tracrRNA retaining nucleotides 23 to 48 of the native sequence was capable of supporting robust dual-RNA–guided Cas9-catalyzed DNA cleavage (Fig. 3, A and C, and fig. S10, A and B). Truncation of the crRNA from either end showed that Cas9-catalyzed cleavage in the presence of tracrRNA could be triggered with crRNAs missing the 3′-terminal 10 nucleotides (Fig. 3, B and C). In contrast, a 10-nucleotide deletion from the 5′ end of crRNA abolished DNA cleavage by Cas9 (Fig. 3B). We also analyzed Cas9 orthologs from various bacterial species for their ability to support *S. pyogenes* tracrRNA:crRNA-guided DNA cleavage. In contrast to closely related *S. pyogenes* Cas9 orthologs, more distantly related orthologs were not functional in the cleavage reaction (fig. S11). Similarly, *S. pyogenes* Cas9 guided by tracrRNA:crRNA duplexes originating from more distant systems was unable to cleave DNA efficiently (fig. S11). Species specificity of dual-RNA–guided cleavage of DNA indicates coevolution of Cas9, tracrRNA, and the crRNA repeat, as well as the existence of a still unknown structure and/or sequence in the dual-RNA that is critical for the formation of the ternary complex with specific Cas9 orthologs.

To investigate the protospacer sequence requirements for type II CRISPR/Cas immunity in bacterial cells, we analyzed a series of protospacer-containing plasmid DNAs harboring single-nucleotide mutations for their maintenance following transformation in *S. pyogenes* and their ability to be cleaved by Cas9 in vitro. In contrast to point mutations introduced at the 5′ end of the protospacer, mutations in the region close to the PAM and the Cas9 cleavage sites were not tolerated in vivo and resulted in decreased plasmid cleavage efficiency in vitro (Fig. 3D). Our results are in agreement with a previous report of protospacer escape mutants selected in the type II CRISPR system from *S. thermophilus* in vivo (*27*, *29*). Furthermore, the plasmid maintenance and cleavage results hint at the existence of a "seed" region located at the 3′ end of the protospacer sequence that is crucial for the interaction with crRNA and subsequent cleavage by Cas9. In support of this notion, Cas9 enhanced complementary DNA strand hybridization to the crRNA; this enhancement was the strongest in the 3′-terminal region of the crRNA targeting sequence (fig. S12). Corroborating this finding, a contiguous stretch of at least 13 base pairs between the crRNA and the target DNA site proximal to the PAM is required for efficient target cleavage, whereas up to six contiguous mismatches in the 5′-terminal region of the protospacer are tolerated (Fig. 3E). These findings are reminiscent of the previously observed seed-sequence requirements for target nucleic acid recognition in Argonaute proteins

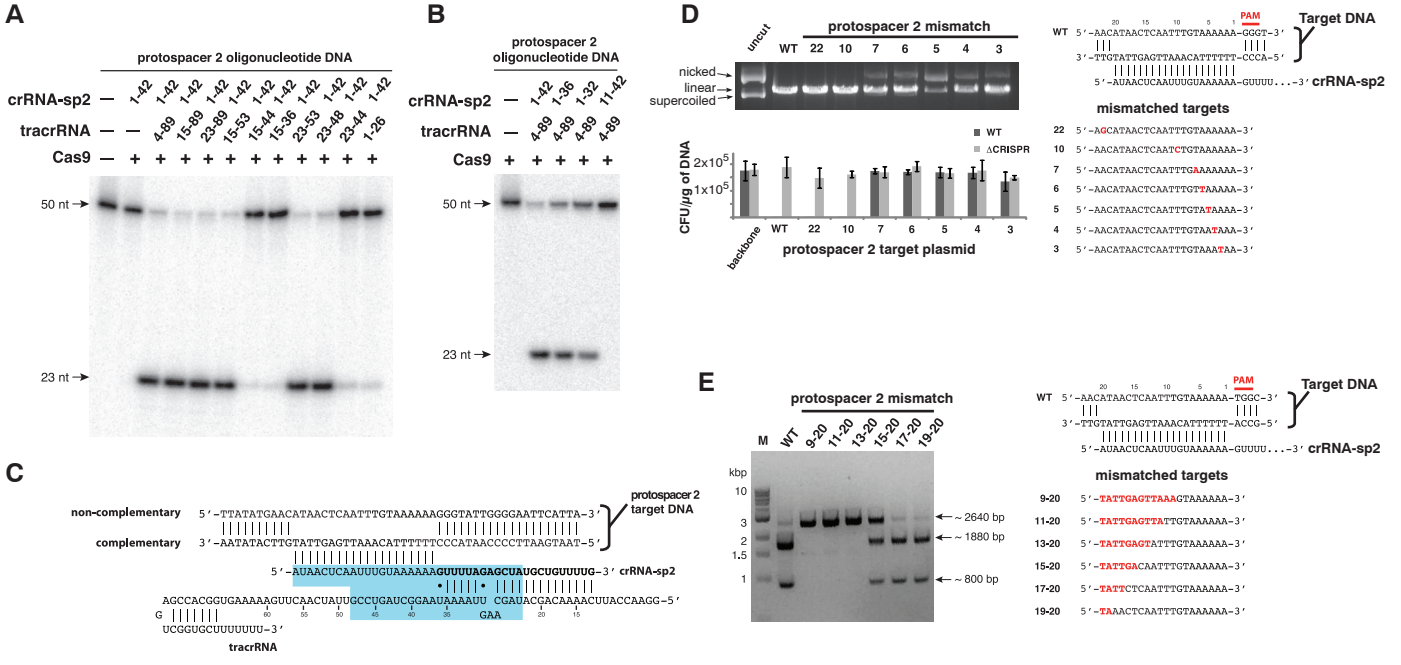

Fig. 3. Cas9-catalyzed cleavage of target DNA requires an activating domain in tracrRNA and is governed by a seed sequence in the crRNA. (**A**) Cas9-tracrRNA:crRNA complexes were reconstituted using 42-nucleotide crRNA-sp2 and truncated tracrRNA constructs and were assayed for cleavage activity as in Fig. 1B. (**B**) Cas9 programmed with full-length tracrRNA and crRNA-sp2 truncations was assayed for activity as in (A). (**C**) Minimal regions of tracrRNA and crRNA capable of guiding Cas9-mediated DNA cleavage (blue shaded region). (**D**) Plasmids containing WT or mutant protospacer 2 sequences with indicated point mutations (right) were cleaved in vitro by programmed Cas9 as in Fig. 1A (top-left) and used for transformation assays of WT or pre-crRNA–deficient *S. pyogenes* (bottom-left). The transformation efficiency was calculated as colony-forming units (CFU) per microgram of plasmid DNA. Error bars represent SDs for three biological replicates. (**E**) Plasmids containing WT and mutant protospacer 2 inserts with varying extent of crRNA-target DNA mismatches (right) were cleaved in vitro by programmed Cas9 (left). The cleavage reactions were further digested with XmnI. The 1880- and 800-bp fragments are Cas9-generated cleavage products. M, DNA marker.

(*30*, *31*) and the Cascade and Csy CRISPR complexes (*13*, *14*).

A short sequence motif dictates R-loop formation. In multiple CRISPR/Cas systems, recognition of self versus nonself has been shown to involve a short sequence motif that is preserved in the foreign genome, referred to as the PAM (*27*, *29*, *32*–*34*). PAM motifs are only a few base pairs in length, and their precise sequence and position vary according to the CRISPR/Cas system type (*32*). In the *S. pyogenes* type II system, the PAM conforms to an NGG consensus sequence, containing two G:C base pairs that occur one base pair downstream of the crRNA binding sequence, within the target DNA (*4*). Transformation assays demonstrated that the GG motif is essential for protospacer plasmid DNA elimination by CRISPR/Cas in bacterial cells (fig. S13A), consistent with previous observations in *S. thermophilus* (*27*). The motif is also essential for in vitro protospacer plasmid cleavage by tracrRNA:crRNA-guided Cas9 (fig. S13B). To determine the role of the PAM in target DNA cleavage by the Cas9-tracrRNA:crRNA complex, we tested a series of dsDNA duplexes containing mutations in the PAM sequence on the complementary or noncomplementary strands, or both (Fig. 4A). Cleavage assays using these substrates showed that Cas9-catalyzed DNA cleavage was particularly sensitive to mutations in the PAM sequence on the noncomplementary strand of the DNA, in contrast to complementary strand PAM recognition by type I CRISPR/Cas systems (*18*, *34*). Cleavage of target single-stranded DNAs was unaffected by mutations of the PAM motif. This observation suggests that the PAM motif is required only in the context of target dsDNA and may thus be required to license duplex unwinding, strand invasion, and the formation of an R-loop structure. When we used a different crRNA-target DNA pair (crRNA-sp4 and protospacer 4 DNA), selected due to the presence of a canonical PAM not present in the protospacer 2 target DNA, we found that both G nucleotides of the PAM were required for efficient Cas9-catalyzed DNA cleavage (Fig. 4B and fig. S13C). To determine whether the PAM plays a direct role in recruiting the Cas9-tracrRNA:crRNA complex to the correct target DNA site, we analyzed binding affinities of the complex for target DNA sequences by native gel mobility shift assays (Fig. 4C). Mutation of either G in the PAM sequence substantially reduced the affinity of Cas9-tracrRNA:crRNA for the target DNA. This finding argues for specific recognition of the PAM sequence by Cas9 as a prerequisite for target DNA binding and possibly strand separation to allow strand invasion and R-loop formation, which would be analogous to the PAM sequence recognition by CasA/Cse1 implicated in a type I CRISPR/Cas system (*34*).

Cas9 can be programmed with a single chimeric RNA. Examination of the likely secondary structure of the tracrRNA:crRNA duplex (Figs. 1E and 3C) suggested the possibility that the features required for site-specific Cas9-catalyzed DNA cleavage could be captured in a single chimeric RNA. Although the tracrRNA:crRNA

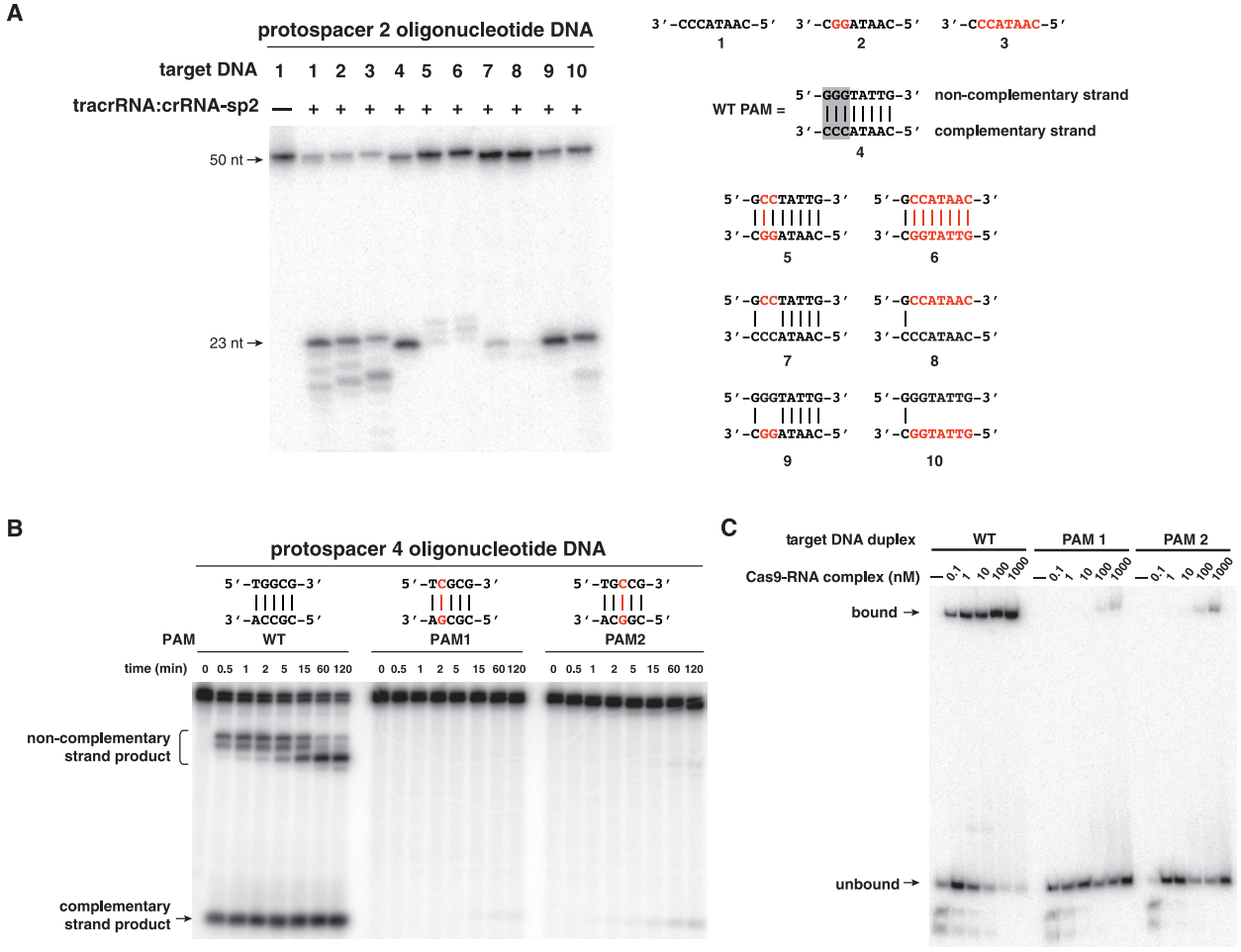

Fig. 4. A PAM is required to license target DNA cleavage by the Cas9-tracrRNA:crRNA complex. (**A**) Dual RNA-programmed Cas9 was tested for activity as in Fig. 1B. WT and mutant PAM sequences in target DNAs are indicated (right). (**B**) Protospacer 4 target DNA duplexes (labeled at both 5′ ends) containing WT and mutant PAM motifs were incubated with Cas9 programmed with tracrRNA:crRNA-sp4 (nucleotides 23 to 89). At the indicated time points (in minutes), aliquots of the cleavage reaction were taken and analyzed as in Fig. 1B. (**C**) Electrophoretic mobility shift assays were performed using RNA-programmed Cas9 (D10A/H840A) and protospacer 4 target DNA duplexes [same as in (B)] containing WT and mutated PAM motifs. The Cas9 (D10A/H840A)–RNA complex was titrated from 100 pM to 1 μM.

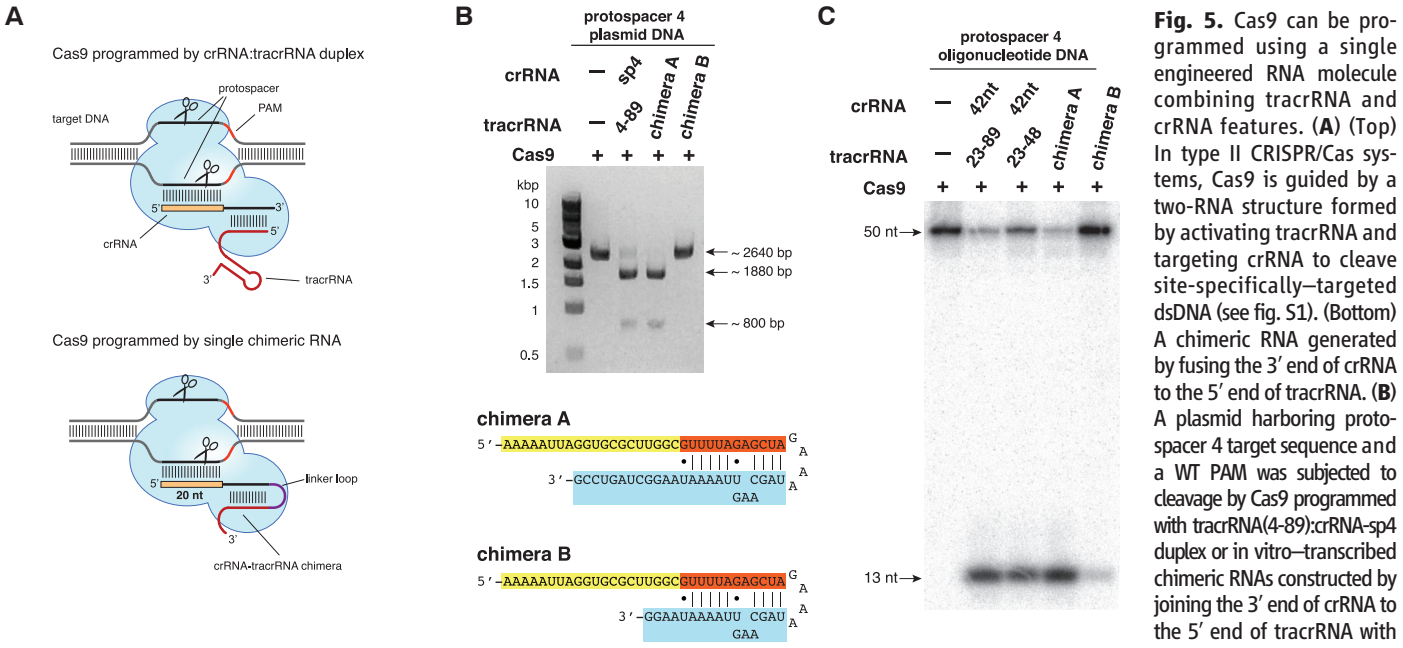

Fig. 5. Cas9 can be programmed using a single engineered RNA molecule combining tracrRNA and crRNA features. (**A**) (Top) In type II CRISPR/Cas systems, Cas9 is guided by a two-RNA structure formed by activating tracrRNA and targeting crRNA to cleave site-specifically–targeted dsDNA (see fig. S1). (Bottom) A chimeric RNA generated by fusing the 3′ end of crRNA to the 5′ end of tracrRNA. (**B**) A plasmid harboring protospacer 4 target sequence and a WT PAM was subjected to cleavage by Cas9 programmed with tracrRNA(4-89):crRNA-sp4 duplex or in vitro–transcribed chimeric RNAs constructed by joining the 3′ end of crRNA to the 5′ end of tracrRNA with a GAAA tetraloop. Cleavage reactions were analyzed by restriction mapping with XmnI. Sequences of chimeric RNAs A and B are shown with DNA-targeting (yellow), crRNA repeat-derived sequences (orange), and tracrRNA-derived (light blue) sequences. (**C**) Protospacer 4 DNA duplex cleavage reactions were performed as in Fig. 1B. (**D**) Five chimeric RNAs designed to target the GFP gene were used to program Cas9 to cleave a GFP gene–containing plasmid. Plasmid cleavage reactions were performed as in Fig. 3E, except that the plasmid DNA was restriction mapped with AvrII after Cas9 cleavage.

target-selection mechanism works efficiently in nature, the possibility of a single RNA-guided Cas9 is appealing due to its potential utility for programmed DNA cleavage and genome editing (Fig. 5A). We designed two versions of a chimeric RNA containing a target recognition sequence at the 5′ end followed by a hairpin structure retaining the base-pairing interactions that occur between the tracrRNA and the crRNA (Fig. 5B). This single transcript effectively fuses the 3′ end of crRNA to the 5′ end of tracrRNA, thereby mimicking the dual-RNA structure required to guide site-specific DNA cleavage by Cas9. In cleavage assays using plasmid DNA, we observed that the longer chimeric RNA was able to guide Cas9-catalyzed DNA cleavage in a manner similar to that observed for the truncated tracrRNA:crRNA duplex (Fig. 5B and fig. S14, A and C). The shorter chimeric RNA did not work efficiently in this assay, confirming that nucleotides that are 5 to 12 positions beyond the tracrRNA:crRNA base-pairing interaction are important for efficient Cas9 binding and/or target recognition. We obtained similar results in cleavage assays using short dsDNA as a substrate, further indicating that the position of the cleavage site in target DNA is identical to that observed using the dual tracrRNA:crRNA as a guide (Fig. 5C and fig. S14, B and C). Finally, to establish whether the design of chimeric RNA might be universally applicable, we engineered five different chimeric guide RNAs to target a portion of the gene encoding the green-fluorescent protein (GFP) (fig. S15, A to C) and tested their efficacy against a plasmid carrying the GFP coding sequence in vitro. In all five cases, Cas9 programmed with these chimeric RNAs efficiently cleaved the plasmid at the correct target site (Fig. 5D and fig. S15D), indicating that rational design of chimeric RNAs is robust and could, in principle, enable targeting of any DNA sequence of interest with few constraints beyond the presence of a GG dinucleotide adjacent to the targeted sequence.

Conclusions. We identify a DNA interference mechanism involving a dual-RNA structure that directs a Cas9 endonuclease to introduce site-specific double-stranded breaks in target DNA. The tracrRNA:crRNA-guided Cas9 protein makes use of distinct endonuclease domains (HNH and RuvC-like domains) to cleave the two strands in the target DNA. Target recognition by Cas9 requires both a seed sequence in the crRNA and a GG dinucleotide-containing PAM sequence adjacent to the crRNA-binding region in the DNA target. We further show that the Cas9 endonuclease can be programmed with guide RNA engineered as a single transcript to target and cleave any dsDNA sequence of interest. The system is efficient, versatile, and programmable by changing the DNA target-binding sequence in the guide chimeric RNA. Zinc-finger nucleases and transcription-activator–like effector nucleases have attracted considerable interest as artificial enzymes engineered to manipulate genomes (*35*–*38*). We propose an alternative methodology based on RNA-programmed Cas9 that could offer considerable potential for gene-targeting and genome-editing applications.

References and Notes

1. B. Wiedenheft, S. H. Sternberg, J. A. Doudna, *Nature* **482**, 331 (2012).
2. D. Bhaya, M. Davison, R. Barrangou, *Annu. Rev. Genet.* **45**, 273 (2011).
3. M. P. Terns, R. M. Terns, *Curr. Opin. Microbiol.* **14**, 321 (2011).
4. E. Deltcheva *et al.*, *Nature* **471**, 602 (2011).
5. J. Carte, R. Wang, H. Li, R. M. Terns, M. P. Terns, *Genes Dev.* **22**, 3489 (2008).
6. R. E. Haurwitz, M. Jinek, B. Wiedenheft, K. Zhou, J. A. Doudna, *Science* **329**, 1355 (2010).
7. R. Wang, G. Preamplume, M. P. Terns, R. M. Terns, H. Li, *Structure* **19**, 257 (2011).
8. E. M. Gesner, M. J. Schellenberg, E. L. Garside, M. M. George, A. M. Macmillan, *Nat. Struct. Mol. Biol.* **18**, 688 (2011).
9. A. Hatoum-Aslan, I. Maniv, L. A. Marraffini, *Proc. Natl. Acad. Sci. U.S.A.* **108**, 21218 (2011).
10. S. J. J. Brouns *et al.*, *Science* **321**, 960 (2008).
11. D. G. Sashital, M. Jinek, J. A. Doudna, *Nat. Struct. Mol. Biol.* **18**, 680 (2011).
12. N. G. Lintner *et al.*, *J. Biol. Chem.* **286**, 21643 (2011).

13. E. Semenova *et al.*, *Proc. Natl. Acad. Sci. U.S.A.* **108**, 10098 (2011).
14. B. Wiedenheft *et al.*, *Proc. Natl. Acad. Sci. U.S.A.* **108**, 10092 (2011).
15. B. Wiedenheft *et al.*, *Nature* **477**, 486 (2011).
16. C. R. Hale *et al.*, *Cell* **139**, 945 (2009).
17. J. A. L. Howard, S. Delmas, I. Ivančić-Baće, E. L. Bolt, *Biochem. J.* **439**, 85 (2011).
18. E. R. Westra *et al.*, *Mol. Cell* **46**, 595 (2012).
19. C. R. Hale *et al.*, *Mol. Cell* **45**, 292 (2012).
20. J. Zhang *et al.*, *Mol. Cell* **45**, 303 (2012).
21. K. S. Makarova *et al.*, *Nat. Rev. Microbiol.* **9**, 467 (2011).
22. K. S. Makarova, N. V. Grishin, S. A. Shabalina, Y. I. Wolf, E. V. Koonin, *Biol. Direct* **1**, 7 (2006).
23. K. S. Makarova, L. Aravind, Y. I. Wolf, E. V. Koonin, *Biol. Direct* **6**, 38 (2011).
24. S. Gottesman, *Nature* **471**, 588 (2011).
25. R. Barrangou *et al.*, *Science* **315**, 1709 (2007).
26. J. E. Garneau *et al.*, *Nature* **468**, 67 (2010).
27. R. Sapranauskas *et al.*, *Nucleic Acids Res.* **39**, 9275 (2011).
28. G. K. Taylor, D. F. Heiter, S. Pietrokovski, B. L. Stoddard, *Nucleic Acids Res.* **39**, 9705 (2011).
29. H. Deveau *et al.*, *J. Bacteriol.* **190**, 1390 (2008).
30. B. P. Lewis, C. B. Burge, D. P. Bartel, *Cell* **120**, 15 (2005).
31. G. Hutvagner, M. J. Simard, *Nat. Rev. Mol. Cell Biol.* **9**, 22 (2008).
32. F. J. M. Mojica, C. Díez-Villaseñor, J. García-Martínez, C. Almendros, *Microbiology* **155**, 733 (2009).
33. L. A. Marraffini, E. J. Sontheimer, *Nature* **463**, 568 (2010).
34. D. G. Sashital, B. Wiedenheft, J. A. Doudna, *Mol. Cell* **46**, 606 (2012).
35. M. Christian *et al.*, *Genetics* **186**, 757 (2010).
36. J. C. Miller *et al.*, *Nat. Biotechnol.* **29**, 143 (2011).
37. F. D. Urnov, E. J. Rebar, M. C. Holmes, H. S. Zhang, P. D. Gregory, *Nat. Rev. Genet.* **11**, 636 (2010).
38. D. Carroll, *Gene Ther.* **15**, 1463 (2008).

Acknowledgments: We thank K. Zhou, A. M. Smith, R. Haurwitz and S. Sternberg for excellent technical assistance; members of the Doudna and Charpentier laboratories and J. Cate for comments on the manuscript; and B. Meyer and T.-W. Lo (Univ. of California, Berkeley/HHMI) for providing the GFP plasmid. This work was funded by the HHMI (M.J. and J.A.D.), the Austrian Science Fund (grant W1207-B09; K.C. and E.C.), the Univ. of Vienna (K.C.), the Swedish Research Council (grants K2010-57X-21436-01-3 and 621-2011-5752-LiMS; E.C.), the Kempe Foundation (E.C.), and Umeå University (K.C. and E.C.). J.A.D. is an Investigator and M.J. is a Research Specialist of the HHMI. K.C. is a fellow of the Austrian Doctoral Program in RNA Biology and is cosupervised by R. Schroeder. We thank A. Witte, U. Bläsi, and R. Schroeder for helpful discussions, financial support to K.C., and for hosting K.C. in their laboratories at MFPL. M.J., K.C., J.A.D., and E.C. have filed a related patent.

Supplementary Materials

www.sciencemag.org/cgi/content/full/science.1225829/DC1
Materials and Methods
Figs. S1 to S15
Tables S1 to S3
References (*39*–*47*)

8 June 2012; accepted 20 June 2012
Published online 28 June 2012;
10.1126/science.1225829

Long-Range Incommensurate Charge Fluctuations in (Y,Nd)$Ba_2Cu_3O_{6+x}$

G. Ghiringhelli,[1]* M. Le Tacon,[2] M. Minola,[1] S. Blanco-Canosa,[2] C. Mazzoli,[1] N. B. Brookes,[3] G. M. De Luca,[4] A. Frano,[2,5] D. G. Hawthorn,[6] F. He,[7] T. Loew,[2] M. Moretti Sala,[3] D. C. Peets,[2] M. Salluzzo,[4] E. Schierle,[5] R. Sutarto,[7,8] G. A. Sawatzky,[8] E. Weschke,[5] B. Keimer,[2]* L. Braicovich[1]

The concept that superconductivity competes with other orders in cuprate superconductors has become increasingly apparent, but obtaining direct evidence with bulk-sensitive probes is challenging. We have used resonant soft x-ray scattering to identify two-dimensional charge fluctuations with an incommensurate periodicity of ~3.2 lattice units in the copper-oxide planes of the superconductors (Y,Nd)$Ba_2Cu_3O_{6+x}$, with hole concentrations of 0.09 to 0.13 per planar Cu ion. The intensity and correlation length of the fluctuation signal increase strongly upon cooling down to the superconducting transition temperature (T_c); further cooling below T_c abruptly reverses the divergence of the charge correlations. In combination with earlier observations of a large gap in the spin excitation spectrum, these data indicate an incipient charge density wave instability that competes with superconductivity.

A successful theory of high-temperature superconductivity in the copper oxides requires a detailed understanding of the spin, charge, and orbital correlations in the normal state from which superconductivity emerges. In recent years, evidence of ordering phenomena in which these correlations might take on particularly simple forms has emerged (*1*, *2*). Despite intense efforts, however, only two order parameters other than superconductivity have thus far been unambiguously identified by bulk-sensitive experimental probes: (i) uniform antiferromagnetism in undoped insulating cuprates and (ii) uniaxially modulated antiferromagnetism (*3*) combined with charge order (*3*, *4*) in doped cuprates of the so-called "214" family [that is, compounds of composition $La_{2-x-y}(Sr,Ba)_x(Nd,Eu)_yCuO_4$]. The latter is known as "stripe order," with a commensurate charge modulation of period 4*a* (where lattice unit a = 3.8 to 3.9 Å is the distance between neighboring Cu atoms in the CuO_2 planes), which greatly reduces the superconducting transition temperature (T_c) of 214 materials at a doping level $p \sim 1/8$ per planar Cu atom. Incommensurate spin fluctuations in 214 materials with $p \neq 1/8$ (*5*) have been interpreted as evidence of fluctuating stripes (*6*). A long-standing debate has evolved around the questions of whether stripe order is a generic feature of the copper oxides and whether stripe fluctuations are essential for superconductivity.

Recent attention has focused on the "123" family [$RBa_2Cu_3O_{6+x}$ with R = Y or another rare earth element], which exhibits substantially lower chemical disorder and higher maximal T_c than the 214 system. For underdoped 123 compounds, the anomaly in the T_c-versus-p relation at $p = 1/8$ (*7*) and the large in-plane anisotropies in the transport properties (*8*, *9*) have been interpreted as evidence of stripe order or fluctuations, in analogy to stripe-ordered 214 materials (*10*). Differences in the spin dynamics of the two families have, however, cast some doubt on this interpretation. In particular, neutron-scattering studies of moderately doped 123 compounds have revealed a gap of magnitude ≥20 meV in the magnetic excitation spectrum (*11*–*14*), whereas 214 compounds with similar hole concentrations exhibit nearly gapless spin excitations (*5*). Further questions have been raised by the recent discovery of small Fermi surface pockets in quantum oscillation experiments on underdoped 123 materials in magnetic fields large enough to weaken or obliterate superconductivity (*15*). Some researchers have attributed this observation to a Fermi surface reconstruction due to magnetic field–induced stripe order (*10*), whereas others have argued that even the high magnetic fields applied in these experiments appear incapable of closing the spin gap and that a biaxial charge modulation is required to explain the quantum oscillation data (*16*). Nuclear magnetic resonance (NMR) experiments have shown evidence of a magnetic field–induced uniaxial charge modulation (*17*), but they do not yield information about electronic fluctuations outside of a very narrow energy window of ~1 μeV. On the other hand, scattering experiments to determine

[1]CNR-SPIN, Consorzio Nazionale Interuniversitario per le Scienze Fisiche della Materia, and Dipartimento di Fisica, Politecnico di Milano, Piazza Leonardo da Vinci 32, I-20133 Milano, Italy. [2]Max-Planck-Institut für Festkörperforschung, Heisenbergstraße 1, D-70569 Stuttgart, Germany. [3]European Synchrotron Radiation Facility (ESRF), BP 220, F-38043 Grenoble Cedex, France. [4]CNR-SPIN, Complesso Monte Sant'Angelo–Via Cinthia, I-80126 Napoli, Italy. [5]Helmholtz-Zentrum Berlin für Materialien und Energie, Albert-Einstein-Straße 15, D-12489 Berlin, Germany. [6]Department of Physics and Astronomy, University of Waterloo, Waterloo, Ontario N2L 3G1, Canada. [7]Canadian Light Source, University of Saskatchewan, Saskatoon, Saskatchewan S7N 0X4, Canada. [8]Department of Physics and Astronomy, University of British Columbia, Vancouver, British Columbia V6T 1Z4, Canada.

*To whom correspondence should be addressed. E-mail: giacomo.ghiringhelli@fisi.polimi.it (G.G.); b.keimer@fkf.mpg.de (B.K.)